Crimson Publishers
Wings to the Research

Review Article

A Short Update on the Nitrogen Reduction Reaction Catalysts for Ammonia Synthesis at Room Temperature

Federico Roncaroli[1,2,3]*

[1]Instituto de Nanociencia y Nanotecnología (CNEA-CONICET), Centro Atómico Constituyentes, Avenida General Paz 1499, (1650) San Martín, Buenos Aires, Argentina

[2]Laboratorio Argentino de Haces de Neutrones, Comisión Nacional de Energía Atómica, Avenida General Paz 1499, (1650) San Martín, Buenos Aires, Argentina

[3]Departamento de Química Inorgánica, Analítica y Química Física, Facultad de Ciencias Exactas y Naturales, Universidad de Buenos Aires, Intendente Güiraldes 2160, Ciudad Universitaria, Ciudad de Buenos Aires (1428), Argentina

ISSN: 2576-8840

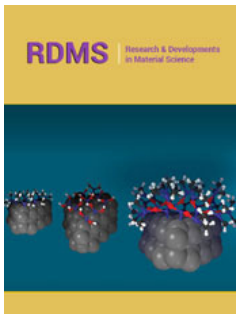

***Corresponding author:** Federico Roncaroli, Instituto de Nanociencia y Nanotecnología (CNEA-CONICET), Laboratorio Argentino de Haces de Neutrones, Centro Atómico Constituyentes, Avenida General Paz 1499, (1650) San Martín, Buenos Aires, Argentina

Submission: March 26, 2025
Published: April 14, 2025

Volume 21 - Issue 4

How to cite this article: Federico Roncaroli. A Short Update on the Nitrogen Reduction Reaction Catalysts for Ammonia Synthesis at Room Temperature. Res Dev Material Sci. 21(4). RDMS. 001016. 2025. DOI: 10.31031/RDMS.2025.21.001016

Abstract

Ammonia production is of fundamental concern because it is required for fertilizers, used in food production and many other applications. However, it relies on the Haber Bosch process, which requires a significant percent of the world energy and is responsible for an important amount of the CO_2 world generation every year. This work tends to summarize the latest results and highest activity catalysts for the Nitrogen Reduction Reaction (NRR) at low temperature. The focus is set on electrochemical NRR, photocatalytic nitrogen fixation and photo electrocatalytic nitrogen reduction. Although an enormous effort was done by the scientific community, the performances of the catalysts are still several orders of magnitude lower from the industrial requirements. The different strategies and materials investigated are analyzed, and new trends and some ideas are proposed. This work tries to be a starting point for those who wish to start working on this fascinating topic of research.

Keywords: Nitrogen fixation; Ammonia synthesis; Electrocatalytic; Photochemical; Photoelectrochemical

Introduction

Ammonia is the main precursor for urea and other nitrogen-containing-fertilizers synthesis, which are essential for agriculture and food production, and for supplying its increasing word demand. Ammonia is also required in the production of a large number of chemicals, including pharmaceuticals, dyes and textiles. Additionally, it has been proposed as a carbon-free fuel [1], due to its high energy density (13.6GJ m^{-3}) and easy transportation properties (boiling point 33.5 °C) [2]. Ammonia is produced industrially mainly through the Haber-Bosch process since more than 100 years ago (1909). In this process, a mixture of N_2 and H_2 react under high pressure and temperature in the presence of a Fe-Mo catalyst (350-550 °C and15-25MPa) [3]. H_2 is obtained principally from natural gas, hence, ammonia production is responsible for the consumption of approximately 1% of this resource, 1.4% of fossil fuels, 2% of global energy, and the 1.6% world CO_2 emission every year [4,5]. Moreover, the NH_3 yield in Haber-Bosch process is less than 15%. For all these reasons, development of processes and catalysts which allow production of ammonia at room temperature and atmospheric pressure or, at least, under more environmental friendly conditions are required, The US Department of Energy has established a target ammonia synthesis rate of $9.3x10^{-7}$mol cm^{-2} s^{-1} for a commercially viable reactor. In turn, as described within this work, most of the reported materials display a catalytic activity orders of magnitude lower [6]. In the last

decades, several strategies and approaches have been employed for this purpose. They will summarized in the present report, focusing on electro-, photo- and photo-electro-catalysis.

NRR technologies

Enzymatic and thermochemical (Haber-Bosch): The ammonia production rate of the native nitrogenase enzymes through the Nitrogen Reduction Reaction (NRR) has been calculated in 30000μmol g^{-1} h^{-1}, the same order of magnitude as the Haber-Bosch process (10000-32000μmol g^{-1} h^{-1}). This rate corresponds to a theoretical limit of ammonia production that could be reached by nitrogenase enzymes [7]. This activity corresponds to purified enzyme using large excess of chemical reducing agents measured *in vitro*, which is dramatically reduced after long-term experiments. The role of ATP during catalytic cycle is still not fully understood. Nitrogenses produce NH_3 under ambient conditions, however, the reaction is still very energy demanding, since it requires 16 ATP molecules per each N_2 reduced molecule. The energy consumption of this enzymatic reaction has been calculated in 13GJ ton^{-1}, not so smaller than the 28GJ ton^{-1} consumed by the Haber-Bosch process [7].

Electrocatalytic NRR: In electrochemical reactions, electricity flows through a cell composed of two electrodes: cathode and anode, where reduction and oxidation reactions take place, respectively. The electrodes are immersed in an electrolyte and, additionally, a reference electrode is usually employed [3]. The NRR is thermodynamically favorable ($E^o(N_2/NH_3)$ = +0.55V vs NHE). However, the high triple bond energy (941kJ mol^{-1}), endothermic protonation enthalpy (941kJ mol^{-1}), high ionization energy (15.8eV), negative electron affinity (-1.9eV) and large energy gap (10.8eV), make redox and acid/base reactions on this molecule very unfavorable, in other words, a very inert molecule [8].

The mechanisms for the electrochemical NRR have been described in detail in many reviews and they will be only summarized here. The overall reaction consists in three steps: (a) N_2 adsorption, (b) N_2-bond cleavage and hydrogenation, and (c) NH_3 desorption. Considering the different sequence of the hydrogenation process and the cleavage of the N_2 triple bond, the mechanisms can be classified into: (i) associative, and (ii) dissociative. In the dissociative mechanism, the N_2 molecule is adsorbed on the catalyst surface and the triple bond is cleaved before the hydrogenation takes place. In turn, in the associative mechanism, hydrogenation occurs during N_2 bond cleavage. The associative mechanism can be classified into (iii) distal and (iv) alternating pathways. In the distal pathway, the remote N-atom is hydrogenated and released as NH_3. On the other hand, in the alternating pathway, both N-atoms are hydrogenated simultaneously and two NH_3 molecules are released sequentially. The rate determining step in the associative mechanism is not the N_2 bond cleavage, what greatly reduces the activation energy. The Haber-Bosch process follows a dissociative mechanism, while the electrocatalytic NRR usually follows associative mechanisms. In the (iv) enzymatic mechanism, both N-atoms bind to the surface in a "side- on" mode, in contrast to the other associative mechanisms, in which the N_2 molecules bind through only one of the N-atoms, in an "end-on" mode, and is the preferred mechanism in most heterogeneous NRR catalysts. Finally, in transition-metal nitrides, the (v) Mars-van Krevelen (MvK) mechanism has been proposed and supported by DFT calculations and quantitative $^{14}N/^{15}N$ isotope exchange experiments. In such mechanisms, N-vacancies play a key role [8-10].

NH_3 detection and quantitation is very critical to obtain reproducible results, including separation from NH_3 impurities from reactants and the atmosphere, since NH_3 concentration produced is very low. Several analytical techniques have been employed, including spectrophotometric (Nessler or Indophenol blue reactions), potentiometric, spectroscopic (NMR) and chromatographic methods, which are described elsewhere [11].

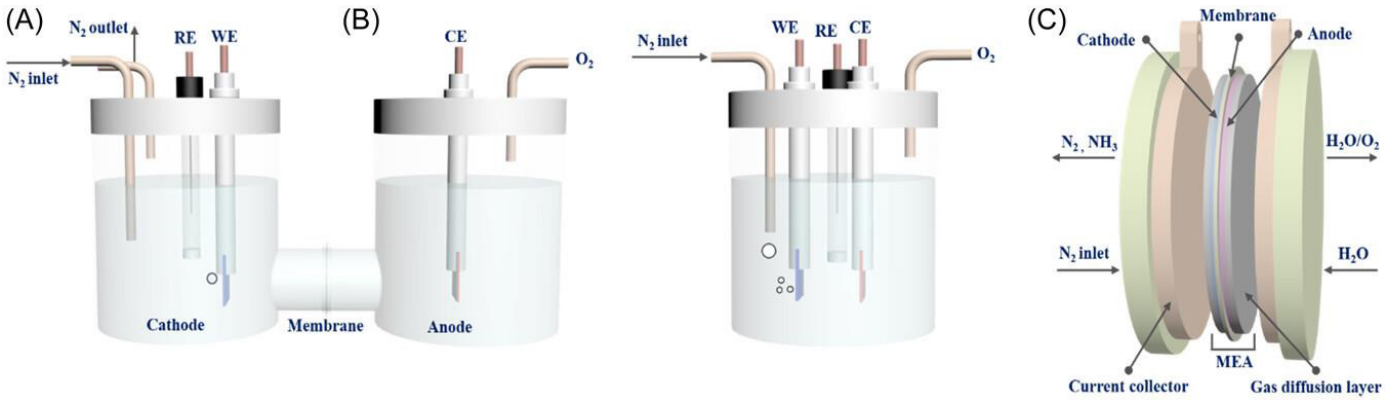

Figure 1: Electrochemical cells for the NRR. (A) H-type cell, (B) single-chamber cell, and (C) MEA-based cell. Reproduced from Ref [12]. Copyright © 2023 Chebrolu, Jang, Rani, Lim, Yong and Kim. This is an open-access article distributed under the terms of the Creative Commons Attribution License (CC BY 4.0 https://creativecommons.org/licenses/by/4.0/).

Electrochemical cells employed in activity tests are shown in Figure 1, and they can be divided into four groups: (i) single chamber cells, where both cathodic and anodic reactions take place in the same chamber-solution without separation. The

NH_3 produced on the cathode can be oxidized on the anode. On the other hand, O_2 produced on the anode may interfere with the NRR. (ii) H-cell, where the cathodic and anodic reactions occur in solutions connected by a tube divided by a membrane or separator. (iii) Polymer-electrolyte- membrane cell (PEM-cell), where the anodic and cathodic solutions are placed in two different chambers separated by a proton exchange membrane [3]. (iv) MEA-based-cells (Membrane-electrode-assemble) are similar to PEM-cells, but N_2 and H_2O are directed separately through gas diffusion layers to the cathode and anode respectively, separated by a PEM-membrane. Reactions occur at the triple phase zone (gas, liquid, solid) on each electrode. The reduced distance between electrodes (zero gap) minimizes the device resistance [12]. (v) Flow cells, similar to PEM-cells, allow *in-situ* monitoring product concentrations (GC-MS) or sample extraction to be analyzed (NMR, UPLC-MS) [13]. Flow cells offer a solution to the low solubility of N_2 in water and allow easy harvest of NH_3 from the cathode [14].

Strategies to improve the catalysts: Catalytic heterogeneous reactions take place on the catalyst surfaces. In this way, defects, vacancies, exposed crystal facet, extrinsic atoms, etc, change the coordination, exposure and electronic structure of active sites, and N_2/intermediates-adsorption properties, with deep influence on the catalytic activity. In this direction, several strategies have been tested: surface engineering, single atom coordination, heteroatom doping, metal oxide deposition, amorphization, [8], structural and strain engineering [10], defect engineering: oxygen-nitrogen- and sulfur-vacancies [15]. Employing the concept of interface engineering, Graphidiyne nanosheets (GDY) (2D carbon allotrope) were grown on cobalt nitride nanowires reaching a remarkable NH_3 yield rate of 219.72μg h^{-1} mg^{-1} and a faradaic efficiency of 58.60%. DFT calculations showed that the π- system of GDY induced a charge-transfer between GDY and cobalt nitride, promoting the catalytic activity, selectivity and durability (114h) [16].

Metal-free 2D materials are mainly formed by carbon-, boron- and carbon-nitride-based materials [11]. Carbon-based materials and graphene are cheap, have high electrical conductivity and specific surface area, and chemical and physical stability. The possibility to obtain different allotropes (nanotubes, graphene sheets, graphidiyne, etc) allows for obtaining a variety of different materials [17]. Non-metal dopants (B, O, N, S, F and P) modulate the electronic and geometric structures with profound influence in the catalytic activity. Different morphologies like nano-sheets, nanotubes, nano-spheres, C-dots have also been investigated [11]. Boron based materials, like boron-nanosheets, B_4C nanosheets, and alloys of B with P (boron phosphide), N (h-BN, hexagonal boron nitride) or Se have been investigated [4,11].

Carbon based metal- and non-metal-composites have been extensively studied due to high electrical conductivity and stability of the carbonaceous materials, relatively easy procedures for heteroatom doping and carbon-metal/oxide composite synthesis [17].

Metal based catalysts which have been tested are oxides, carbides, nitrides, phosphides, sulfides, selenides, borides, single atom catalysts, layered double hidroxydes (LDH), metal-organic frameworks (MOFs) and MXenes [10,11]. Metal nitrides have been extensively studied through theoretical methods. Such works predicted, in principle, higher activity towards the NRR than HER, due to a mechanism mediated by N-vacancies (Mars-van Krevelen mechanism). However, experimental studies on some metal nitrides resulted in faradaic efficiencies between 1-6% [6]. Recent studies employing in operando near ambient pressure XPS on VN (vanadium nitride) revealed the importance of oxygen atoms on the surface and the difference between N_2(solvated) and N-lattice on the reduction mechanism [18]. In order to prolong the residence time of N_2, increase the collision probability of N_2, and improve the contact between N_2 and active sites, hollow particles have been designed [19].

Single atom catalysts are very attractive due to their maximum atom utilization, novel electronic-geometric structure of the active site, which may be different from its bulk structures, leading to remarkable catalytic performance. This is particularly interesting for scarce and expensive metals. For example, the catalysts Ru/NC and Au_1/C_3N_4 were obtained, which reached the NH_3 yield rates of 3.665mg h^{-1} mg_{Ru}^{-1} and 1305μg h^{-1} mg_{Au}^{-1} respectively [8].

Mo has been extensively studied as catalyst for the NRR, particularly MoS_2 [20]. Theoretical calculations have shown favorable electronic structure for catalysis and particularly for NRR [21]. In fact, natural nitrogenases enzymes have Mo in the active site. The basal plane of MoS_2 could be activated through LiOH treatment (2H-MoS_2(MoS_2), generating pores and exposing active sites. In this way, an impressive activity of 3405.55µgNH_3 mg_{cat}^{-1} h^{-1}; 1.98µg h^{-1} cm^{-2} was reached [22].

Ru is at the top of the Skulasson's volcano diagram for NRR, due to a compromise between nitrogen adsorption energy and overpotential for associative and dissociative mechanisms, being lower than other noble metals like Pt and Pd [21]. In this context, Ru has been employed as part of many different catalysts. A Ru (III) polyethyleneimine (PEI) complex supported on carboxyl-modified carbon nanotubes (Ru (III)-PEI@MWCNTs) reached a NH_3 yield rate of 188.90µgNH_3 mg_{cat}^{-1} h^{-1} and a faradaic efficiency of 30.93% (-0.1V vs RHE) [23].

A 3D Covalent Organic Framework (COF) with Fe-N_4 catalytic sites (Fe@NUST-18) has been obtained from condensation between 5,10,15,20-tetrayl(tetrakis(([1,1':3',1''-terphenyl]-4,4''-dicarbaldehyde)))-porphyrin (TTEP) and quadrilateral 1,2,4,5-tetrakis-(4-aminophenyl) benzene (TAPB). The NH3 yield rate and the Faradaic efficiency were 94.26 ± 4.9µg h^{-1} mg^{-1} and 18.37 % at -0.5V vs RHE. These values were higher than the corresponding ones for the Cu analogue, evidencing the superior activity of Fe catalysts towards the NRR [24].

Dual atom catalysts: Exploiting the properties of some metals like Mo and Fe, which have strong binding energies towards N, and Co which binds N weakly, bimetallic catalysts have been developed with increased activity [6]. Dual-single-atom catalysts have the advantage of possessing abundant active sites and the possibility to act synergically between them, what might improve selectivity, N_2 adsorption, activation, and hydrogenation [25,26].

MOFs, Metal organic frameworks are porous, crystalline, 2D- or 3D-coordination polymers with organic ligands, [27]. MOFs and their derivatives have been evaluated as electrocatalysts for NRR, following several strategies, including Mo and Ru doping, reaching activities up to 100μg h^{-1} mg^{-1} [28,29]. The roles of defects have been thoroughly studied and characterized [30]. A remarkable case corresponds to a F-doped carbon obtained from pyrolysis of a mixture of UiO-66 and poly(tetrafluoroethylene) (PTFE) followed by HF leaching to remove ZrO_2 produced during the pyrolysis. The NH_3 yield rate reached 197.7μgNH_3 mg^{-1}_{cat} h^{-1} and a faradaic efficiency of 54.8% at -0.2V vs RHE. The author suggested that F acting as Lewis acid suppressed H binding and the Hydrogen Evolution Reaction (HER), enhancing in this way the selectivity towards NRR [31].

MXenes are 2D transition-metal carbides/nitrides/carbonitrides, they have the general formula $M_{n+1}X_nT_x$ (M = transition metal, X = C or N or both), T terminal group = OH, O, F, Cl). They show good hydrophilicity, large specific surface area, high electrical conductivity (usually metallic) and abundant active sites. They are susceptible for post-functionalization, co-catalyst loading, generating derived-and composite-materials. [32,33]. Other 2D materials relevant for the NRR are layered double hydroxides and bismuth-based layered materials [34]. The last ones will be discussed later in the photocatalytic section.

Competing reactions: N_2H_4 formation and the Hydrogen Evolution Reaction (HER). NRR requires six protons and six electrons per N_2 molecule, in contrast, HER requires only two protons and two electrons, what envisions that HER will be more favorable in most catalysts. Hence, the HER is the most competitive reaction against NRR. Several strategies have been tested and recently reviewed. These strategies include limiting the proton accessibility or proton donor concentration, building a hydrophobic protection layer on the catalyst surface, limiting the electron accessibility, increasing the reaction pressure, changing the reaction temperature [10,14]. The hydrophilicity/hydrophobicity of the catalyst/electrolyte interface has deep influence on the NRR/HER selectivity, since it can control the accessibility of protons to the surface [14]. Interestingly, potassium and other alkaline ions have shown suppression effect on the HER due to competition with protons [35]. Other strategies include catalyst design: Early-transition-metal catalysts, atomically dispersed catalysts, support with low HER activity, introduction of species with low HER activity [10]. N_2H_4 is formed as intermediate in some mechanisms of NRR. Since it usually has low affinity for the active sites, it is not a serious competitor against the NRR.

Organic solvents: low-proton concentration or hybrid electrolytes consist of mixtures of proton donors (water, alcohols, pyridines, etc.) and aprotic solvents (DMSO, THF, etc). They allow control the proton concentration and suppress the HER, increasing the selectivity for NRR [14].

Ionic liquids exhibit high N_2 solubility and have been evaluated as electrolytes. They managed to achieve a high conversion efficiency of 60% for N_2 electro-reduction to ammonia on a nanostructured iron catalyst under ambient conditions [36].

Protonic ceramic electrolysis cells (PCECs) for ammonia (NH_3) synthesis have been developed, and they are other alternatives to the use of water and organic solvents. The highest reported rate was 14×10^{-9}mol cm^{-2} s^{-1} [37]. There are proton conducting ceramic membranes: Yb_2O_3 doped $SrCeO_3$, Sm_2O_3 doped $BaCeO_3$, Gd_2O_3 doped CeO_2 (600-750 °C) [38], which could be also tested for NRR catalysis.

Metal-N_2 batteries have been design, employing NRR catalysts on the cathodes. Several metals were evaluated as well as aqueous or organic electrolytes. Maximum power densities were about 4900Wh kg^{-1} (Na metal, α-MnO_2 nanowire, 1 M $NaCF_3SO_3$/ TEGDME solution), 2.6mW cm^{-2} (Al metal MoPi/HSNPC, 1.0M KOH) [39].

Li mediated electrochemical NRR, consists in the formation of Li nitride upon direct reaction of N_2 with Li, followed by electrochemical Li(metal) recovery. This technique will not be discussed in this report and the reader is directed to more specialized literature [40].

Table 1 shows some recent results on electrocatalytic NRR catalysts, focusing on the most active and efficient ones [41-46].

Table 1: Some resent results on high activity and efficiency catalysts for electrochemical NRR.

Catalyst	Faraday Efficiency	NH_3 Formation Rate	Conditions	Ref
BiNCs	66%	200 mmol g^{-1} h^{-1} (0.052 mmol cm^{-2} h^{-1})	-0.6V vs RHE, 0.5 mol^{-1} of K_2SO_4, pH 3.5	[35]
$Nb_3O_7(OH)$/CFC	39.9 %	622μg h^{-1} mg_{cat}^{-1}	-0.4V 0.1M Na_2SO_4	[41]
GDY/Co2N	58.60 %	219.72μg h^{-1} mg_{cat}^{-1}	-0.2V 0.1M HCl	[16]
SAB/C	71 %	$(9.5\pm0.4) \times 10^{-10}$ mol s^{-1} cm^{-2}	10M LiCl	[42]
$Cu_3(HITP)_2$@h-BN)	42.5 %	146.2μg h^{-1} mg_{cat}^{-1}	-0.3V vs RHE	[43]
CuO NWAs	95.8 %	0.2449mmol h^{-1} cm^{-2}	0.5m Na_2SO_4	[44]
F-doped carbon	54.3	197.7μg h^{-1} mg_{cat}^{-1}	- 0.3/-0.2V vs RHE 0.05M H_2SO_4	[31]
ECOF@BCP (COF)	54.5 %	287.2μg h^{-1} mg_{cat}^{-1}		[45]
PCN-222(Fe)	70.7%	110.9μg h^{-1} mg_{cat}^{-1}	0.1 M HCl	[46]
2H-MoS_2(PAL-MoS_2)	44.36 %	3405.55μgNH_3 mg_{cat}^{-1} h^{-1} (1.98μg h^{-1} cm^{-2})	-0.1V	[22]

Photocatalytic nitrogen fixation: Upon light absorption by a semiconductor material, electrons are promoted from the valence band to the conduction band, while holes remain in the valence band. Electrons, which do not recombine with holes, could migrate to the semiconductor surface and reduce N_2. The holes, on the other hand, will oxidize H_2O to O_2 or some sacrificial reducing agent (Figure 2). The mechanism involves several steps required for the electron-hole-pair photo-generation and separation, before the adsorbed N_2 is actually reduced. Photocatalytic nitrogen fixation experiments are typically performed in a suspension of the catalyst in water, in a vessel or reactor transparent to light. Although it is a very environmentally friendly strategy, there are difficulties in separating the reduction (NH_3) and oxidation (O_2, etc.) products of the photocatalytic reactions. More over, the produced NH_3 can be oxidized during the reaction. This last drawback can be solved by photo-electro-catalysis, which will be discussed in the following section [34].

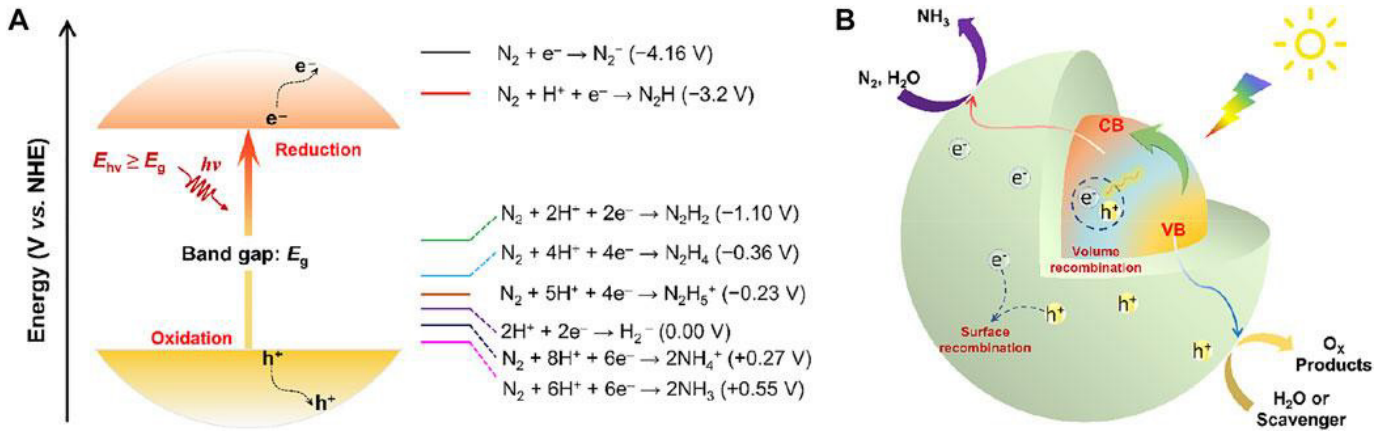

Figure 2: (A) Schematic energy diagram related to the reduction of N_2 to NH_3. (B) Schematic illustration of the complete photocatalytic NH3 synthesis over semiconductor-based photocatalysts. Reproduced from Ref [61]. Copyright © 2022 Hui, Wang, Yao, Hao and Sun. This is an open-access article distributed under the terms of the Creative Commons Attribution License (CC BY 4.0). https://creativecommons.org/licenses/by/4.0/

Many metal oxides and calcogenides have been used as substrates for photocatalytic nitrogen reduction, taking advantage of the suitable band gap energy and presence of d- orbitals able to interact with N_2 molecules, for example: BiO, TiO_2, Fe_2O_3, Cu_2O, Ga_2O_3, ZnO, MoO_2, WO_3, MoS_2, etc [47]. In order to facilitate charge transfer, avoid electron-hole recombination and increase photocatalytic efficiency, several strategies have been exercised which include p-n junctions, Z-schemes, s-schemes, single atom catalysts, vacancy and doping engineering (O, N, S, etc), co-catalyst promotion, and surface plasmon resonance [47]. Graphitic carbon nitride, g-C_3N_4, which has been extensively used as photocatalyst for many reactions due to its n-type semiconductor nature, chemical and thermal stability, has also been employed as composite in photo-NRR [47]. Moreover, N- vacancies (NV) can be generated, which provide very specific sites for N adsorption.

Bi based materials are very promising photocatalysts due to: high abundance in nature, their employ in various fields like CO_2 reduction and H_2 production, and strong chemical interaction with N_2 *via* electron donation from p orbitals. In this way, several Bi oxides, oxihalides and mix-oxides with W and Mo have been investigated. Several strategies were tested, including the "bismuth rich" strategy [5]. Highly dispersed bismuth sulfide was grown on a Zr tetracarbxyphenyl porphyrine MOF (Bi_2S_3@PCN-2). A N-fixation rate of 3880μg h^{-1} g^{-1} was reached. The high specific surface area and porosity of the MOF allowed the N adsorption and activation while preventing Bi_2S_3 nanorod aggregation. Additionally, the high-density heterojunctions improved substantially the charge transfer rate and separation efficiency of photogenerated electrons and holes [48].

Metal-Organic Frameworks (MOFs), which hold high density of metallic centers, high specific surface area, crystalline structures and high porosity, have also been tested as photocatalysts [49]. MOFs can directly adsorb N_2 through the π-antibonding activation mechanism. Alternatively, N_2 absorption and subsequent reduction may be induced upon ligand to metal charge transfer after photon absorption by the ligands [49].

MOFs have some disadvantages like low electrical conductivity and low stability under catalytic conditions. However, the integration with other materials, particularly semiconductors, producing composites, can help to resolve these problems. Zn-MOF-74 was deposited on a g-C_3N_4 film generating a Z-scheme heterjunction composite, which reached a Nitrogen fixation activity of 2.32mmol g^{-1} h^{-1}. Ru-doped In_2O_3 hollow peanuts were obtained from pyrolysis of MIL-68-In(Ru), yielding a photocatalytic nitrogen fixation activity of 44.5mmol $g^{-1}h^{-1}$ [49].

A ternary TiO_2/MIL-88A(Fe)/g-C_3N_4 heterojunction was constructed through hydrothermal synthesis. The yield of NH_3 rate reached 1084.31μmol g^{-1} h^{-1} under simulated sunlight illumination in methanol water solution. The yield was more than 10 times higher than the separated components. DFT calculations supported a Z-scheme mechanism, which resulted in improved photo-induced charge separation and transfer [50].

Covalent-Organic Frameworks (COFs) have also been investigated as photocatalysts for NRR, particularly as supports of single atoms catalysts (SACs). COFs have the advantage, like MOFs, of having ordered porous structures suitable for gas absorption and diffusion, aromatic rings allowing UV-vis and even NIR light absorption, functional groups capable to coordinate metallic ions and generate SACs. For example, the COF5-Au reached a NH3 evolution performance with the rate of 427.9μmol g^{-1} h^{-1} [51].

Plasmonic Au metallic nanoparticles were confined and dispersed within the pores of a MOF (UiO-66) membrane. Through the surface plasmon resonance (LSPR), hot electrons were generated upon light harvesting and were transferred to the N_2 molecules adsorbed on the Au nanoparticles. The evanescent surface plasmon resonance field further activated the N_2 molecules as well, resulting in a supralinear intensity dependence of the NH_3 evolution rate [52].

Table 2 summarizes some recent results on N_2-photofixation [53-61].

Table 2: Photocatalytic nitrogen fixation catalysts.

Catalyst	NH_3 formation rate	Conditions	Ref
Cu_2O	4.1mmol h^{-1} g^{-1} (0.14 %)	300 W Xe lamp, 800 - 400nm	[53]
ZnO-Ni_xPy	2304μmol g^{-1} h^{-1}	50W Hg lamp	[54]
Pd-EG-BiOBr	2492.6μmol g^{-1} h^{-1}	300W Xe lamp, MeOH 2%	[55]
Sn-doped MOF-5	3912.76μmol L^{-1} g^{-1}	300W Xe lamp, 5hs	[56]
g-C_3N_4/MoS_2/$PbTiO_3$	6288μmol L^{-1} g^{-1} h^{-1}	300W Xe lamp	[57]
TiO_2 QDs modified by Bi_2O_3/$NaBiS_2$	8704μmol L^{-1} g^{-1}	500W Xe lamp	[58]
MOF-74@C_3N_4	2320μmol g^{-1} h^{-1}	Xenon Lamp (300w) λ>400 nm, ethanol	[59]
MIL-68-In(Ru) hollow peanuts	4450μmol g^{-1} h^{-1}	AM 1.5, ethanol	[60]
BiS@PCN-2	3880μg h^{-1} g^{-1}	Bisphenol A	[48]
Au@UiO-66	18.9mmol gAu^{-1} h^{-1} (1.54%)	>400nm, 100mW cm^{-2}	[52]

Photoelectrochemical NRR: Both electrical and light energy are employed to accomplish the reaction. In general the band gap energy or the energy transition between the highest occupied molecular orbital and the lowest unoccupied molecular orbital, are not high enough to drive the NRR and the application of a potential bias is necessary. In order to improve the efficiency, photocathodes have been constructed, employing a p-type semiconductor (for example: p-Si, p-$BiVO_4$, Cu_2O, BiOI) which supports the NRR catalyst [62]. Three steps occur during photo-electro-catalysis: (i) light absorption by the photocathode and generation of the photo-induced electron-hole pairs. (ii) Diffusion and separation of electron-hole pairs. (iii) Migration of electrons to the active sites, where NRR takes place, and migration of the holes to the counter electrode, where oxidation of water or other sacrificial reducing agents occurs. Photo-electro-catalysis has the advantage of separation of the reactions products in two different chambers of the cell, and improvement of the reduction/oxidation abilities of photo-excited electrons/holes for the desired reactions through application of a potential bias [63]. p-$BiVO_4$ has been very popular as photocatalyst, moreover V-sites are very active towards NRR [62].

Some sophisticated strategies from photocatalysis have been also tested. A Z-scheme heterojuction has been constructed employing a $BiVO_4$/polyaniline junction, in which, the staggered band structure of the materials permitted separation and acceleration of the holes and electrons. A hetero-structure with a double electron-transfer mechanism was built with NV-g-C_3N_5 and BiOBr. (NV = N-vacancies) (29.4μg h^{-1} mg^{-1}, 11% at -0.2V) [62].

A cascade n+np+-Si photocathode coupled to a Au/porous carbon nitride (PCN) catalyst was built aiming to decouple the light harvesting and the electrocatalysis. DFT calculations showed that the porous structure and N-vacancies of the catalyst facilitated N_2 adsorption. This strategy allowed reaching a faradic efficiency of 61.8% and a NH_3 production yield of 13.8μg h^{-1} cm^{-2} at −0.10V vs RHE [64].

Black phosphor has relatively low activity towards HER, what makes a good candidate for NRR catalysis. A photocathode was built depositing layer by layer black phosphor on an indium tin oxide substrate, reaching a remarkable 102.4μg h^{-1} mg_{cat}^{-1} NH production rate with a Faradaic efficiency of 23.3% [4,62,65]. Some recent results on photo electrocatalysts for the NRR are summarized in Table 3. As a comparison, it is possible to observe that the electrocatalytic NRR has the highest efficiency, while the photocatalytic one has the lowest, reaching the photo-electro-catalytic technology intermediate efficiencies [66,67]; Figure 3.

Table 3: Some results on photo-electrochemical nitrogen reduction.

Catalyst	Efficiency	NH_3 formation rate	Conditions	Ref.
BP (black phosphor)	23.3% at -0.4V	102.4μg h^{-1} mg_{cat}^{-1}	Hg/Xe lamp; HCl	[65]
NVs g-C_3N_5/ BiOBr	11% at - 0.2V	29.4μg h^{-1} mg^{-1}	1 sun illumination, HCl-Na_2SO_4	[66]
Vo-BiOBr/ TiO_2	----	25.08μg h^{-1} cm^{-2}	Xe lamp, Na_2SO_4	[67]
n+np+-Si /Au/PCN	61.8% at -0.V vs RHE	13.8μg h^{-1} cm^{-2}		[64]

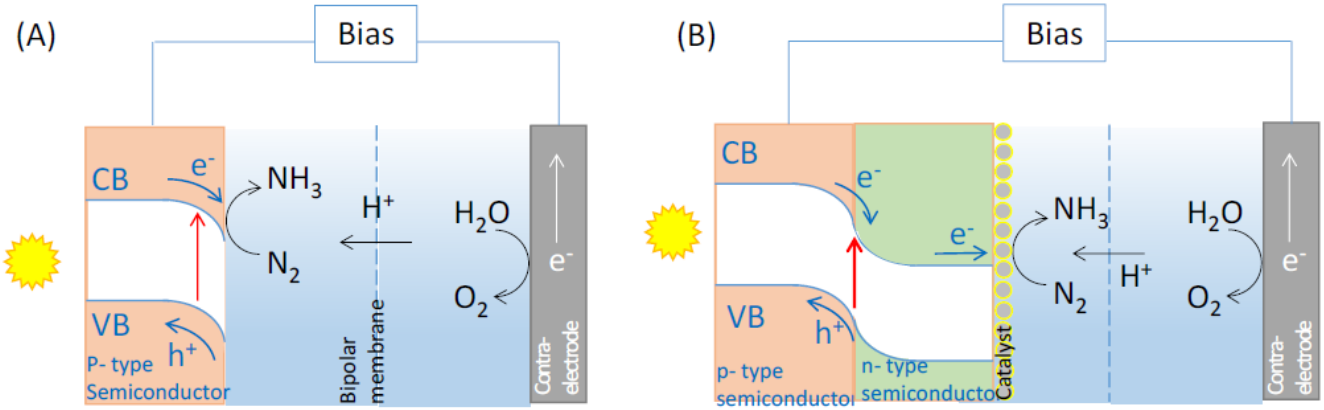

Figure 3: Schematic representation of a photo-electro-catalytic cell for NH_3 synthesis, showing qualitatively the band energy diagram of the photocathode. (A) Simplest model, where a p-type semiconductor is employed as photocathode. (B). Catalysts particles are grown on a n-p heterojunction photocathode.

Conclusions and Perspectives

Although a huge effort to obtain highly active catalysts, following many different strategies, and deeper understanding of their mechanisms have been made, NRR catalytic activities are still orders of magnitude lower than industrial requirements. It has been proposed that at least a NH_3 yield of 6120μg h^{-1} cm^{-2}, a faraday efficiency of 50% and current density of 300mA cm^{-2} are needed for industrial application [3]. Protons are, on one hand, reactants for the NRR and on the other hand competitors due to the HER. Unfortunately, the selectivity of most of the catalysts is still low.

Single atom catalysts are promising towards the NRR. In most of these materials, metal sites are N-coordinated and were obtained from pyrolysis of MOFs or organic molecules [27-29]. This brings the consequence of low single-atom concentration and high heterogeneity and disorder of the catalyst structure. In this way COFs and nitrogenated organic polymers could be an alternative. Mo based electron conductive COFs and MOFs have been predicted as highly active catalysts towards the NRR [68-70].

Biological nitrogenase enzymes exhibit activities similar to the ones of the Haber-Bosch process, however, their mechanism and structure are still not fully understood. Deeper understanding of these enzymes would be necessary in order to design new materials and catalysts, which can mimic more accurately their action. A better understanding of the proton delivery and accessibility to the active sites, and how the HER is suppressed, should help to reach higher NH_3 yields, efficiencies and selectivity.

In situ and *in operando* spectroscopic techniques should be more often employed, like near ambient pressure XPS [10], Raman (SERS), infrared (DRIFTS, SEIRAS, ATR-FTIR) and X-ray absorption spectroscopies (XANES, EXASFS), which allow detection of intermediates at the same time as their evolution. This would improve our knowledge of the nature and structure of reaction intermediates and have a deeper understanding of the mechanisms. Another modern technique is the Steady State Isotopic Transient Kinetic Analysis (SSITKA), in which the reactor is coupled to a mass spectrometer or an infrared spectrometer, to study the $^{15}N/^{14}N$ isotopic analysis of the reaction products in the gas phase or the catalysis surface, respectively. This technique allows obtaining information about the catalysis nature [71], and design new ones with improved activity.

Improved computational calculations and machine learning, with the availability of large data bases [72] are expected to give clues or help to discover new materials with higher activity and to approach the industry requirements [4]. As already discussed DFT calculations are performed for the NRR on a particular catalyst surface, but very few investigate a larger number of materials, in order to obtain trends and predictions that can guide the development of new catalysts [3].

In summary, research on NRR catalysts has seen an enormous growth with the design synthesis of a great variety of new materials and catalysts and new understanding of the mechanisms. However, the yields are still low to meet the industrial application. Many new strategies are tested in order to face this problem from different approaches. There is no doubt that exciting new results will come in the short future that will help to solve this problem definitely.

Declaration of Competing Interest

The author declares that there are no known competing financial interests or personal relationships that could have appeared to influence the work reported in this paper.

Acknowledgements

This work was supported by the Research Council of Argentina (CONICET), and the Commission for Atomic Energy of Argentina (CNEA). The author is a researcher of both CONICET and CNEA.

References

1. David WIF, Agnew GD, Bañares-Alcántara R, Barth J, Bøgild Hansen J, et al. (2024) 2023 roadmap on ammonia as a carbon-free fuel. J Phys Energy 6: 21501.

2. Zheng J, Jiang L, Lyu Y, Jiang SP, Wang S (2022) Green synthesis of nitrogen-to- ammonia fixation: Past, present, and future. ENERGY Environ Mater 5: 452-457.

3. Zhao X, Hu G, Chen GF, Zhang H, Zhang S, Wang H (2021) Comprehensive understanding of the thriving ambient electrochemical nitrogen reduction reaction. Adv Mater 33: 2007650.

4. Liu C, Tian A, Li Q, Wang T, Qin G, et al. (2023) 2D, metal-free electrocatalysts for the nitrogen reduction reaction. Adv Funct Mater 33: 2210759.

5. Sun Y, Ahmadi Y, Kim KH, Lee J (2022) The use of bismuth-based photocatalysts for the production of ammonia through photocatalytic nitrogen fixation. Renew Sustain Energy Rev 170: 112967.

6. Ceballos BM, Pilania G, Ramaiyan KP, Banerjee A, Kreller C, et al. (2021) Roads less traveled: Nitrogen reduction reaction catalyst design strategies for improved selectivity. Curr Opin Electrochem 28: 100723.

7. Rapson TD, Wood CC (2022) Analysis of the ammonia production rates by nitrogenase. Catalysts 12(8): 844.

8. Guo D, Wang S, Xu J, Zheng W, Wang D (2022) Defect and interface engineering for electrochemical nitrogen reduction reaction under ambient conditions. J Energy Chem 65: 448-468.

9. Shetty AU, Sankannavar R (2024) Exploring nitrogen reduction reaction mechanisms in electrocatalytic ammonia synthesis: A comprehensive review. J Energy Chem 92:681-697.

10. Mushtaq MA, Arif M, Yasin G, Tabish M, Kumar A, et al. (2023) Recent developments in heterogeneous electrocatalysts for ambient nitrogen reduction to ammonia: Activity, challenges, and future perspectives. Renew Sustain Energy Rev 176: 113197.

11. Liu D, Chen M, Du X, Ai H, Lo KH, et al. (2021) Development of electrocatalysts for efficient nitrogen reduction reaction under ambient condition. Adv Funct Mater 31: 2008983.

12. Chebrolu VT, Jang D, Rani GM, Lim C, Yong K, et al. (2023) Overview of emerging catalytic materials for electrochemical green ammonia synthesis and process. Carbon Energy 5: e361.

13. Feng D, Zhou L, White TJ, Cheetham AK, Ma T, et al. (2023) Nanoengineering metal-organic frameworks and derivatives for electrosynthesis of ammonia. Nano-Micro Lett 15: 203.

14. Ren Y, Yu C, Tan X, Huang H, Wei Q, et al. (2021) Strategies to suppress hydrogen evolution for highly selective electrocatalytic nitrogen reduction: challenges and perspectives. Energy Environ Sci 14:1176-1193.

15. Xu Y, Liu X, Cao N, Xu X, Bi L (2021) Defect engineering for electrocatalytic nitrogen reduction reaction at ambient conditions. Sustain Mater Technol 27: e00229.

16. Fang Y, Xue Y, Li Y, Yu H, Hui L, et al. (2020) Graphdiyne interface engineering: highly active and selective ammonia synthesis. Angew Chemie Int Ed 59: 13021-13027.

17. Zhao Y, Yan L, Zhao X (2022) Development of carbon-based electrocatalysts for ambient nitrogen reduction reaction: challenges and perspectives. Chem Electro Chem 9: e202101126.

18. Balogun K, Ganesan A, Chukwunenye P, Gharaee M, Adesope Q, et al. (2023) Vanadium oxide, vanadium oxynitride, and cobalt oxynitride as electrocatalysts for the nitrogen reduction reaction: a review of recent developments. J Phys Condens Matter 35: 333002.

19. Xue C, Zhou X, Li X, Yang N, Xin X, et al. (2022) Rational synthesis and regulation of hollow structural materials for electrocatalytic nitrogen reduction reaction. Adv Sci 9: 2104183.

20. Guo X, Wan X, Shui J (2021) Molybdenum-based materials for electrocatalytic nitrogen reduction reaction. Cell Reports Phys Sci 2: 100447.

21. Akter R, Shah SS, Ehsan MA, Shaikh MN, Zahir MH, et al. (2024) Transition-metal-based catalysts for electrochemical synthesis of ammonia by nitrogen reduction reaction: Advancing the green ammonia economy. Chem - An Asian J 19: e202300797.

22. Chen J, Zhang C, Huang M, Zhang J, Zhang J, et al. (2021) The activation of porous atomic layered MoS_2 basal-plane to induce adjacent Mo atom pairs promoting high efficiency electrochemical N_2 fixation. Appl Catal B Environ 285: 119810.

23. Xu GR, Batmunkh M, Donne S, Jin H, Jiang JX, et al. (2019) Ruthenium(iii) polyethyleneimine complexes for bifunctional ammonia production and biomass upgrading. J Mater Chem A 7:25433-25440.

24. Shan Z, Sun Y, Wu M, Zhou Y, Wang J, et al. (2024) Metal- porphyrin-based three-dimensional covalent organic frameworks for electrocatalytic nitrogen reduction. Appl Catal B Environ 342: 123418.

25. Liang M, Shao X, Lee H (2024) Recent developments of dual single-atom catalysts for nitrogen reduction reaction. Chem - A Eur J 30: e202302843.

26. Hamsa AP, Unni SM (2024) Electrocatalytic nitrogen reduction reaction: recent advances in dual-atom catalysts for sustainable ammonia production. Catal Sci Technol 14: 3820-3837.

27. Han B, Liu J, Lee C, Lv C, Yan Q (2023) Recent advances in metal-organic framework-based nanomaterials for electrocatalytic nitrogen reduction. Small Methods 7: 2300277.

28. He H, Wen HM, Li HK, Zhang HW (2022) Recent advances in metal-organic frameworks and their derivatives for electrocatalytic nitrogen reduction to ammonia. Coord Chem Rev 471: 214761.

29. Yu Y, Li Y, Fang Y, Wen L, Tu B, et al. (2024) Recent advances of ammonia synthesis under ambient conditions over metal-organic framework based electrocatalysts. Appl Catal B Environ 340: 123161.

30. Khalil IE, Xue C, Liu W, Li X, Shen Y, et al. (2021) The role of defects in metal–organic frameworks for nitrogen reduction reaction: When defects switch to features. Adv Funct Mater 31: 2010052.

31. Liu Y, Li Q, Guo X, Kong X, Ke J, et al. (2020) A highly efficient metal-free electrocatalyst of f-doped porous carbon toward N_2 electroreduction. Adv Mater 32: 1907690.

32. Kok SHW, Lee J, Tan LL, Ong WJ, Chai SP (2022) MXene-A new paradigm toward artificial nitrogen fixation for sustainable ammonia generation: Synthesis, properties, and future outlook. ACS Mater Lett 4: 212-245.

33. Amrillah T, Hermawan A, Alviani VN, Seh ZW, Yin S (2021) MXenes and their derivatives as nitrogen reduction reaction catalysts: recent progress and perspectives. Mater Today Energy 22: 100864.

34. Fu Y, Liao Y, Li P, Li H, Jiang S, et al. (2022) Layer structured materials for ambient nitrogen fixation. Coord Chem Rev 460: 214468.

35. Hao YC, Guo Y, Chen LW, Shu M, Wang XY, et al. (2019) Promoting nitrogen electroreduction to ammonia with bismuth nanocrystals and potassium cations in water. Nat Catal 2: 448-456.

36. Zhou F, Azofra LM, Ali M, Kar M, Simonov AN, et al. (2017) Electro-synthesis of ammonia from nitrogen at ambient temperature and pressure in ionic liquids. Energy Environ Sci 10: 2516-2520.

37. Vieri HM, Kim MC, Badakhsh A, Choi SH (2024) Electrochemical synthesis of ammonia via nitrogen reduction and oxygen evolution reactions-A comprehensive review on electrolyte-supported cells. Energies, p. 17.

38. Giddey S, Badwal SPS, Kulkarni A (2013) Review of electrochemical ammonia production technologies and materials. Int J Hydrogen Energy 38: 14576-14594.

39. Jesudass SC, Surendran S, Kim JY, An TY, Janani G, et al. (2023) Pathways of the electrochemical nitrogen reduction reaction: From ammonia synthesis to metal-N_2 Batteries. Electrochem Energy Rev 6: 27.

40. Jin H, Kim SS, Venkateshalu S, Lee J, Lee K, et al. (2023) Electrochemical

nitrogen fixation for green ammonia: Recent progress and challenges. Adv Sci 10: 2300951.

41. Wu T, Han M, Zhu X, Wang G, Zhang Y, et al. (2019) Experimental and theoretical understanding on electrochemical activation and inactivation processes of $Nb_3O_7(OH)$ for ambient electrosynthesis of NH_3. J Mater Chem A 7: 16969-16978.

42. Wang M, Liu S, Ji H, Yang T, Qian T, et al. (2021) Salting-out effect promoting highly efficient ambient ammonia synthesis. Nat Commun 12: 3198.

43. Liu J, He L, Zhao S, Hu L, Li S, Zhang Z, Du M (2023) A robust n-n heterojunction: Cu and B boosting for ambient electrocatalytic nitrogen reduction to ammonia. Small 19: 2302600.

44. Wang Y, Zhou W, Jia R, Yu Y, Zhang B (2020) Unveiling the activity origin of a copper-based electrocatalyst for selective nitrate reduction to ammonia. Angew Chemie Int Ed 59: 5350-5354.

45. Liu S, Qian T, Wang M, Ji H, Shen X, et al. (2021) Proton-filtering covalent organic frameworks with superior nitrogen penetration flux promote ambient ammonia synthesis. Nat Catal 4: 322-331.

46. He H, Li HK, Zhu QQ, Li CP, Zhang Z, et al. (2022) Hydrophobicity modulation on a ferriporphyrin-based metal-organic framework for enhanced ambient electrocatalytic nitrogen fixation. Appl Catal B Environ 316: 121673.

47. Sun B, Lu S, Qian Y, Zhang X, Tian J (2023) Recent progress in research and design concepts for the characterization, testing, and photocatalysts for nitrogen reduction reaction. Carbon Energy 5: e305.

48. Chen C, Ji R, Xia X, Jin L, Deng K, et al. (2024) Dispersed Bi_2S_3 site in a porphyrin-based metal-organic framework for photocatalytic nitrogen fixation. Appl Energy 357: 122508.

49. Hu K, Huang Z, Zeng L, Zhang Z, Mei L, et al. (2022) Recent advances in mof-based materials for photocatalytic nitrogen fixation. Eur J Inorg Chem 2022: e202100748.

50. Ding Q, Zou X, Ke J, Dong Y, Cui Y, et al. (2023) Enhanced artificial nitrogen fixation efficiency induced by construction of ternary TiO_2/MIL-88A(Fe)/g-C_3N_4 Z- scheme heterojunction. J Colloid Interface Sci 649: 148-158.

51. He T, Zhao Z, Liu R, Liu X, Ni B, et al. (2023) Porphyrin-based covalent organic frameworks anchoring au single atoms for photocatalytic nitrogen fixation. J Am Chem Soc 145: 6057-6066.

52. Chen LW, Hao YC, Guo Y, Zhang Q, Li J, et al. (2021) Metal-Organic framework membranes encapsulating gold nanoparticles for direct plasmonic photocatalytic nitrogen fixation. J Am Chem Soc 143: 5727-5736.

53. Zhang S, Zhao Y, Shi R, Zhou C, Waterhouse GIN, et al. (2021) Sub-3 nm ultrafine Cu_2O for visible light driven nitrogen fixation. Angew Chemie Int Ed 60: 2554-2560.

54. Ray A, Sultana S, Tripathy SP, Parida K (2021) Aggrandizing the Photoactivity of ZnO Nanorods toward N_2 Reduction and H2 Evolution through Facile *In Situ* Coupling with Ni_xP_y. ACS Sustain Chem Eng 9: 6305-6317.

55. Liu J, Li F, Lu J, Li R, Wang Y, et al. (2021) Atomically dispersed palladium-ethylene glycol- bismuth oxybromide for photocatalytic nitrogen fixation: Insight of molecular bridge mechanism. J Colloid Interface Sci 603:17-24.

56. Li L, Lv X, Jin L, Du K, Jiang J, et al. (2024) Facile synthesis of Sn-doped MOF-5 catalysts for efficient photocatalytic nitrogen fixation. Appl Catal B Environ Energy 344: 123586.

57. Dong Z, Feng H, Li L, Hu Y, Yang T, et al. (2023) Photocatalytic nitrogen fixation by g-C_3N_4/MoS_2/$PbTiO_3$ with synergistic electric field. J Alloys Compd 968: 172226.

58. Pournemati K, Habibi YA, Khataee A (2023) Outstanding photocatalytic nitrogen fixation performance of TiO_2 QDs modified by Bi_2O_3/$NaBiS_2$ nanostructures upon simulated sunlight. J Colloid Interface Sci 641: 1000-1013.

59. Ding Z, Wang S, Chang X, Wang DH, Zhang T (2020) Nano-MOF@defected film C_3N_4 Z-scheme composite for visible-light photocatalytic nitrogen fixation. RSC Adv 10: 26246-26255.

60. Vu MH, Quach TA, Do TO (2021) The construction of Ru-doped In_2O_3 hollow peanut-like structure for an enhanced photocatalytic nitrogen reduction under solar light irradiation. Sustain Energy Fuels 5: 2528-2536.

61. Hui X, Wang L, Yao Z, Hao L, Sun Z (2022) Recent progress of photocatalysts based on tungsten and related metals for nitrogen reduction to ammonia. Front Chem 10: 978078.

62. Ješić D, Pomeroy B, Kamal KM, Kovačič Ž, Huš M, et al. (2024) Photo- and photoelectrocatalysis in nitrogen reduction reactions to ammonia: Interfaces, mechanisms, and modeling simulations. Adv Energy Sustain Res 5: 2400083.

63. Guo C, Ran J, Vasileff A, Qiao SZ (2018) Rational design of electrocatalysts and photo(electro)catalysts for nitrogen reduction to ammonia (NH_3) under ambient conditions. Energy Environ Sci 11: 45-56.

64. Peramaiah K, Ramalingam V, Fu HC, Alsabban MM, Ahmad R, et al. (2021) Optically and electrocatalytically decoupled si photocathodes with a porous carbon nitride catalyst for nitrogen reduction with over 61.8% faradaic efficiency. Adv Mater 33: 2100812.

65. Liu D, Wang J, Bian S, Liu Q, Gao Y, et al. (2020) Photoelectrochemical synthesis of ammonia with black phosphorus. Adv Funct Mater 30: 2002731.

66. Li M, Lu Q, Liu M, Yin P, Wu C, et al. (2020) Photoinduced charge separation via the double-electron transfer mechanism in nitrogen vacancies g-C_3N_5/Biobr for the photoelectrochemical nitrogen reduction. ACS Appl Mater Interfaces 12: 38266-38274.

67. Lin S, Chen Y, Fu J, Sun L, Jiang Q, et al. (2022) Photoelectrocatalytic nitrogen fixation with Vo-BiOBr/TiO_2 heterostructured photoelectrode as photocatalyst. Int J Hydrogen Energy 47: 41553-41563.

68. Wang C, Zhao YN, Zhu CY, Zhang M, Geng Y, et al. (2020) A two-dimensional conductive Mo-based covalent organic framework as an efficient electrocatalyst for nitrogen fixation. J Mater Chem A 8: 23599-23606.

69. Sun Y, Shi W, Sun M, Fang Q, Ren X, et al. (2023) Molybdenum based 2D conductive metal-organic frameworks as efficient single-atom electrocatalysts for N_2 reduction: A density functional theory study. Int J Hydrogen Energy 48: 19972-19983.

70. Zhang J, Zhu X, Geng W, Li T, Li M, et al. (2021) $MO_3(C_6X_6)_2$ (X=NH,S,O) Monolayers: Two-dimensional conductive metal-organic frameworks as effective electrocatalysts for the nitrogen reduction reaction. J Energy Chem 61: 71-76.

71. Singh S, Mohammed AK, Al Hammadi AA, Shetty D, Polychronopoulou K (2023) Hypes and hopes on the materials development strategies to produce ammonia at mild conditions. Int J Hydrogen Energy 48: 34700-34739.

72. Dai TY, Wang TH, Wen Z, Jiang Q (2024) Recent progress on computation-Guided catalyst design for highly efficient nitrogen reduction reaction. Adv Funct Mater 34: 2400773.